

FSH Directly Regulates Bone Mass

Li Sun,¹ Yuanzhen Peng,¹ Allison C. Sharrow,^{2,3} Jameel Iqbal,¹ Zhiyuan Zhang,¹ Dionysios J. Papachristou,^{2,3} Samir Zaidi,¹ Ling-Ling Zhu,¹ Beatrice B. Yaroslavskiy,^{2,3} Hang Zhou,¹ Alberta Zallone,⁴ M. Ram Sairam,⁵ T. Rajendra Kumar,⁶ Wei Bo,⁷ Jonathan Braun,⁷ Luis Cardoso-Landa,¹ Mitchell B. Schaffler,¹ Baljit S. Moonga,¹ Harry C. Blair,^{2,3,*} and Mone Zaidi^{1,*}

¹ Mount Sinai Bone Program, Department of Medicine and Department of Orthopedics, Mount Sinai School of Medicine, New York, NY 10029, USA

² Departments of Pathology and Cell Biology, University of Pittsburgh, Pittsburgh, PA 15261, USA

³ VA Medical Center, Pittsburgh, PA 15261, USA

⁴ Department of Anatomy and Histology, University of Bari, 70124 Bari, Italy

⁵ Clinical Research Institute of Montreal, Montreal, QC H2W 1R7, Canada

⁶ Department of Molecular and Integrative Physiology, University of Kansas, Kansas City, KS 66160, USA

⁷ Department of Pathology, University of California, Los Angeles, Los Angeles, CA 90095, USA

*Contact: hclair@imap.upitt.edu (H.C.B.); mone.zaidi@mssm.edu (M.Z.)

DOI 10.1016/j.cell.2006.01.051

SUMMARY

Postmenopausal osteoporosis, a global public health problem, has for decades been attributed solely to declining estrogen levels. Although FSH levels rise sharply in parallel, a direct effect of FSH on the skeleton has never been explored. We show that FSH is required for hypogonadal bone loss. Neither FSH β nor FSH receptor (FSHR) null mice have bone loss despite severe hypogonadism. Bone mass is increased and osteoclastic resorption is decreased in haploinsufficient FSH $\beta^{+/-}$ mice with normal ovarian function, suggesting that the skeletal action of FSH is estrogen independent. Osteoclasts and their precursors possess G_{i2 α} -coupled FSHRs that activate MEK/Erk, NF- κ B, and Akt to result in enhanced osteoclast formation and function. We suggest that high circulating FSH causes hypogonadal bone loss.

INTRODUCTION

Osteoporosis affects nearly 45 million women worldwide with fracture rates that far exceed the combined incidence of breast cancer, stroke, and heart attacks (Stepnick, 2004). The disease results from a disruption of the fine balance between osteoblastic bone formation and osteoclastic bone resorption (Zaidi et al., 1993; Manolagas and Jilka, 1995). After menopause, resorption significantly exceeds formation, and this imbalance results in net bone loss. Estrogen replacement slows postmenopausal bone loss and reduces the risk of fracture (Lindsay, 2004).

In vitro evidence suggests that estrogen inhibits osteoclastic bone resorption by reducing the release of the inflammatory cytokines IL-1, IL-6, and TNF- α from osteoblasts. Similarly, estrogen attenuates and estrogen loss

enhances TNF- α production from T cells (Roggia et al., 2001; Cenci et al., 2003). Estrogen also directly inhibits osteoclast differentiation by acting on bone-marrow precursors (Shevde et al., 2000; Srivastava et al., 2001). Thus, while estrogen is used widely in the therapy of osteoporosis, the primary mechanism of its action at the cellular level remains unclear.

Furthermore, estrogen deficiency itself does not fully explain the bone loss accompanying hypogonadism. An unexpected observation is that mice with both α and β estrogen receptors deleted are only mildly osteopenic, and those null for either receptor have a normal bone mass (McCauley et al., 2002; Windahl et al., 2002; Lindberg et al., 2001). Furthermore, while ovariectomy itself causes profound bone loss, the response is blunted in hypophysectomized rats (Yeh et al., 1996; Yeh et al., 1997). This attests to the requirement of an intact pituitary for a full decrease in bone mass following gonadectomy. In fact, it is the pituitary-derived hormone FSH, rather than serum estrogen, that correlates best with markers of bone turnover in postmenopausal women (Sowers et al., 2003). Similarly, there is a strong correlation between high FSH levels and low bone mass in women with amenorrhea (Devleta et al., 2004). Likewise, decreases in serum FSH levels correlate tightly with gains in bone mass resulting from estrogen therapy (Kawai et al., 2004). These apparent anomalies provide a compelling argument for an alternate, possibly pituitary-driven mechanism for hypogonadal bone loss.

Pituitary-derived hormones were thought to function only through receptors in target endocrine glands (Sairam, 1999). However, we discovered that, apart from stimulating thyroxine secretion, TSH suppressed bone remodeling by acting directly on osteoclasts and osteoblasts (Abe et al., 2003). Deletion of the TSH receptor (TSHR) in mice resulted in high-turnover osteoporosis independent of serum thyroxine levels (Abe et al., 2003), suggesting that a low TSH may contribute to the osteoporosis accompanying hyperthyroidism. Likewise, FSH is considered a primary stimulus for estrogen production from ovarian

follicular cells (Robker and Richards, 1998). As FSH secretion is negatively regulated by estrogenic feedback, a high circulating FSH level invariably accompanies hypogonadism. FSH has thus been regarded as a marker for the onset of menopause (Prior, 1998). However, it has never been tested whether FSH might directly cause the osteoporosis associated with hypogonadism. The results presented here establish that FSH regulates osteoclastic bone resorption and bone mass directly.

RESULTS

Hypogonadal FSH Receptor Null Mice Do Not Lose Bone

Despite severe hypogonadism, we found that *FSHR*^{-/-} mice do not lose bone. With all forms of the *FSHR* deleted, *FSHR*^{-/-} mice exhibit disordered estrous cycles, ovulatory defects, atrophic ovaries, and a thread-like uterus characteristic of severe estrogen deficiency (Figure 1A) (Dierich et al., 1998; Danilovich et al., 2000). Consistent with FSH resistance, circulating FSH levels were higher in *FSHR*^{-/-} mice (mean ± SEM, 44.5 ± 1.40 ng/ml) compared with controls (7.29 ± 2.82, *p* < 0.01). Areal and volumetric BMD at both trabecular and cortical sites in *FSHR*^{-/-} mice were indistinguishable from those of controls (Figures 1B, 1D, and 1E; see also Table S1 in the Supplemental Data available with this article online). No differences were observed in femoral trabecular BV/TV, Tb.Th.3D, or Tb.N on μ CT or histomorphometry (Table 1 and Table S1). In contrast, ovariectomized controls showed a significant (*p* = 0.021) 15% reduction in lumbar spine areal BMD by 8 weeks (Figure 1C). The results indicate that FSH action is necessary for the bone loss associated with hypogonadism.

The resorption marker serum tartrate-resistant acid phosphatase-5b (TRAP) and the formation marker osteocalcin remained indistinguishable between *FSHR*^{+/+} and *FSHR*^{-/-} mice (Figures 1Fa and 1Fb). There were no differences in overall resorption or formation parameters on histomorphometry (Table 1). In contrast, ovariectomized controls had significantly elevated serum TRAP compared with shams (Figure 1Fc). Ex vivo studies revealed a reduction in osteoclastogenic and bone-resorptive activity in *FSHR*^{-/-} cultures compared to controls (Figures 1Ga and 1Gb). Likewise, *TRAP* mRNA expression was reduced (Figure 1H). *TSHR*^{-/-} cultures, in contrast, showed an expected enhancement in *TRAP* mRNA (Figure 1H) (Abe et al., 2003). These differences were not associated with diminished c-Kit⁺/CD11b⁺/c-Fms⁺ pools (Figure 1I). These results indicate that hypogonadism does not alter basal levels of bone resorption or formation in *FSHR*^{-/-} mice.

The discrepancy between normal resorptive surfaces in situ (Table 1) and defective osteoclastogenesis and resorption in vitro (Figure 1G) was examined further by studying the effect of RANK-L on osteoclast numbers in intact calvarial bones using a method modified from Novack et al. (2003). While TRAP-labeled surfaces were not different between *FSHR*^{-/-} and *FSHR*^{+/+} mice, the

enhanced TRAP labeling triggered by RANK-L or FSH in wild-type calvaria was lost in *FSHR*^{-/-} calvaria (Figure 1J). We conclude that the absence of FSH action induces a defect in osteoclastogenesis that is compensated for in vivo but becomes apparent with a proresorptive stimulus.

Eugonadal FSH β Haploinsufficient Mice Have Increased Bone Mass

We hypothesized that FSH β deficiency would conserve bone similarly to *FSHR* deficiency. FSH β homozygous females were sterile and severely hypogonadal with atrophic ovaries and thread-like uteri (Figure 2Aa) (Kumar et al., 1997). Despite this, FSH β ^{-/-} mice did not lose bone; their spinal and tibial areal BMDs were similar to those of wild-type mice (Figure 2B). In fact, at the femur, both areal and volumetric BMD were increased, as were μ CT measures of BV/TV and Tb.N (Figures 2B–2D and Table S1). Thus, as with *FSHR* deletion, FSH β elimination prevented bone loss and even increased bone mass, despite the severe hypogonadism.

Heterozygotic FSH β ^{+/-} mice were eugonadal and fully fertile, with normal ovaries and uteri (Figure 2Aa), but had a 50% reduction in serum FSH levels (Figure 2Ab). This allowed us to examine the effects of FSH independently of estrogen status. FSH haploinsufficiency was associated with an increase in spinal and femoral areal BMD compared with wild-type mice (Figure 2B). At the femoral neck, vBMD, BVF, and Tb.N were also strikingly increased (Figures 2C and 2D and Table S1). Likewise, histomorphometric spinal B.Ar/T.Ar was increased (Table 1). At the femoral diaphysis, there was an increase in cortical thickness (Figures 2C and 2D). These increases were associated with (1) diminished TRAP-labeled resorption surfaces in situ (Table 1), (2) a significant 42% reduction in serum TRAP (Figure 2Ea), and (3) markedly reduced expression of *TRAP*, *cathepsin K*, and *RANK* in bone marrow (Figure 2F). Thus, in mice with a normal estrogen status, lowering circulating FSH by half decreased osteoclast differentiation and bone resorption and increased trabecular number and bone mass. These estrogen-independent actions provide evidence for a direct effect of FSH on the skeleton.

In contrast to bone resorption indices, bone formation parameters, including mineralizing surface and mineral apposition rate, were unchanged in FSH β ^{+/-} mice (Table 1). Consistent with this, no significant differences were noted in serum osteocalcin between the three groups (Figure 2Eb). Furthermore, there were no differences in two- or three-dimensional measures of Tb.Th (Table 1 and Table S1). Thus, the conserved bone mass in FSH β deficiency does not arise from increased bone formation. This is in keeping with our observations on the lack of a direct effect of FSH on osteoblastic bone formation.

FSH Receptors Are Localized to the Osteoclast Surface

FSHR mRNA was detected in primary murine and RAW cell precursors during differentiation (Figures 3Aa and

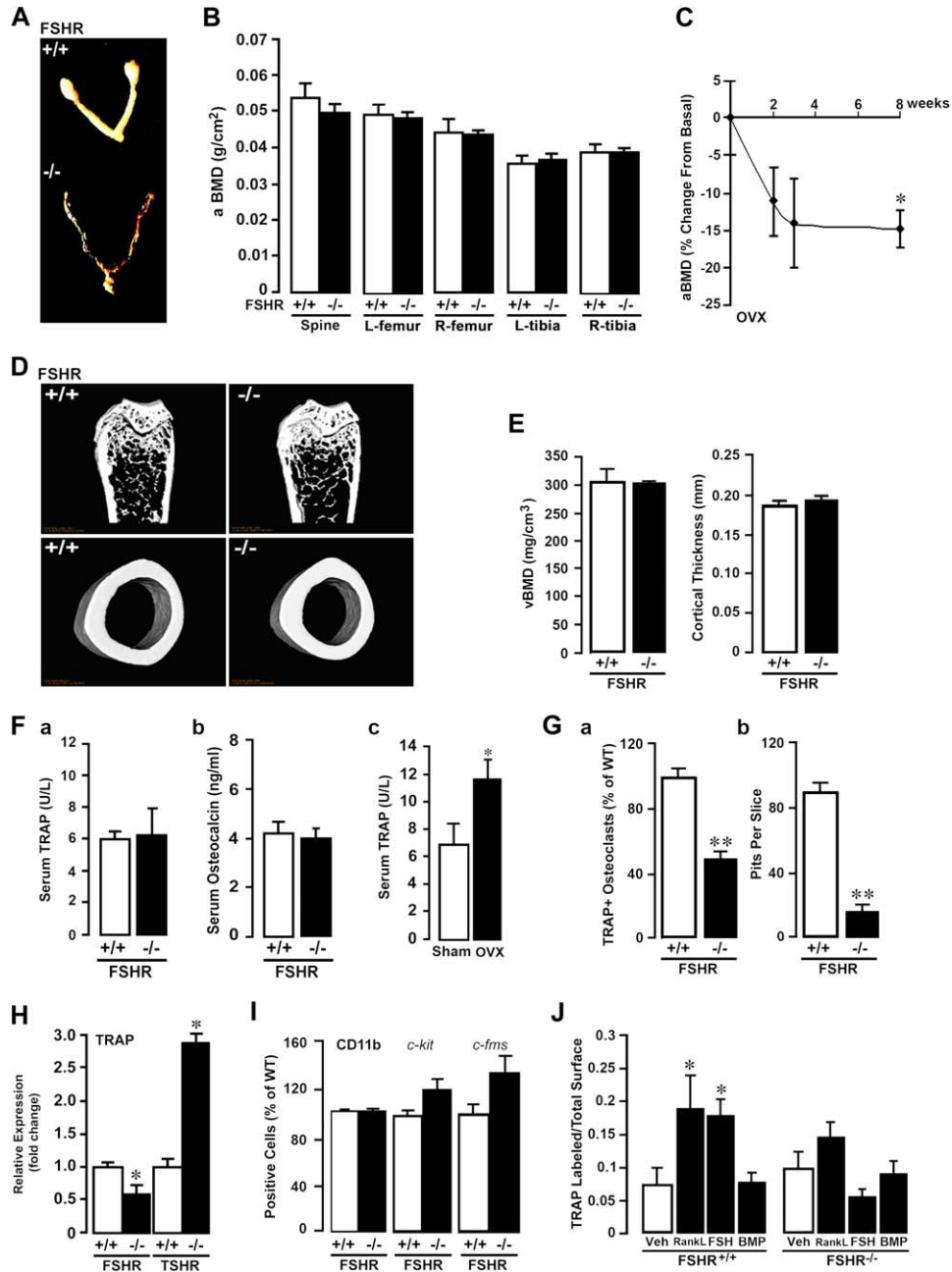


Figure 1. Conserved Bone Mass in Hypogonadal FSHR-Deficient Mice

(A) Hypogonadal FSHR^{-/-} mice have hypoplastic uteri and atrophic ovaries.

(B) Areal bone mineral density (aBMD) in 4-month-old mice. Mean \pm SEM (4–11 mice/group).

(C) Serial lumbar spine aBMDs following ovariectomy (OVX) of wild-type (wt) mice. Mean % change from basal (day 0) \pm SEM (n = 4 mice); p = 0.021.

(D) Frontal (upper) and transverse (lower) μ CT sections of distal femoral and middiaphyses.

(E) Volumetric BMD (vBMD) and cortical thickness at the distal and middiaphyses. Mean \pm SEM (n = 3 mice/group).

(Fa–Fc) Serum TRAP (U/L, Fa and Fc) and osteocalcin (ng/ml, Fb) levels. Mean \pm SEM (5–14 mice/group).

(Ga) TRAP-positive osteoclasts (100 ng/ml RANK-L). % of wt \pm SEM, n = 12 wells/group, two experiments.

(Gb) Bone resorption by osteoclasts. Pits/slice \pm SEM, n = 5 slices, 3 mice/group.

(H) Real-time PCR for TRAP mRNA in bone-marrow cultures (RANK-L, 60 ng/ml) for 5 days. Mean fold change from wt \pm SEM; triplicate; pooled samples; normalized to GAPDH.

(I) FACS comparing cells for CD11b, c-Kit, and c-Fms. % of wt \pm SEM, n = 3 mice/group.

(J) Effect of RANK-L (100 ng/ml), FSH (100 ng/ml), and BMP-2 (200 ng/ml) on TRAP-labeled surfaces/total surface in calvarial bones ex vivo (method modified from Novack et al., 2003). Multiple blinded measurements on three or four bones \pm SEM. *p < 0.05, **p < 0.01.

Table 1. Static and Dynamic Histomorphometry

Parameter (abbreviation)	FSH β			FSHR	
	+/+	+/-	-/-	+/+	-/-
TRAP labeled (%) (Oc.Pm)	25.3 \pm 4.1	18.6 \pm 5.9*	21.3 \pm 7.2*	30.1 \pm 6.4	30.5 \pm 2.1
Trabecular bone area (%) (B.Ar/T.Ar)	26.5 \pm 5.1	35.3 \pm 8.3*	26.5 \pm 2.9	28.2 \pm 13.1	28.8 \pm 12.2
Trabecular thickness (μ m) (Tb.Th)	46.0 \pm 6.8	43.5 \pm 1.7	42.9 \pm 4.3	36.6 \pm 5.0	35.4 \pm 2.7
Mineral apposition rate (μ m/d) (Ir.L.Th/Ir.L.t)	1.41 \pm 0.05	1.41 \pm 0.12	1.45 \pm 0.06	0.90 \pm 0.11	0.93 \pm 0.05

Measurements and calculated parameters in cancellous bone of double-calcein-labeled FSH $\beta^{+/+}$, FSH $\beta^{+/-}$, and FSH $\beta^{-/-}$ mice (6 months old) and FSHR $^{+/+}$ and FSHR $^{-/-}$ mice (4 months old). Measurements are from von Kossa or hematoxylin-and-eosin-stained undecalcified sections by digital measurements of photomicrographs. Mean \pm SD for eight cross-sections from four animals per group is shown. Statistics, unpaired Student's t test, * $p < 0.05$.

3Ab) but not in FSHR $^{-/-}$ osteoclasts (Figure 3Ac). Likewise, RT-PCR using two separate primer sets showed *FSHR* mRNA expression in human osteoclasts and mesenchymal stem cells but not in osteoblasts (Figure 3Ba). These data were confirmed by Affymetrix gene arrays that demonstrated *FSHR* expression in mature osteoclasts ($p = 0.02$) and mesenchymal stem cells ($p = 0.008$) but not in CD14 $^{+}$ precursors ($p = 0.19$), fibroblasts ($p = 0.14$), or mature osteoblasts ($p > 0.1$) (GEO# GPL3327). Western blotting of whole-cell lysates from human osteoclasts, 8 days post-RANK-L, showed an 80 kDa band (Minegishi et al., 1991) (Figure 3Bb) also seen in COV34 ovarian granulosa tumor cells (positive control) and mesenchymal stem cells but not in MG63 cells or mineralizing or quiescent osteoblasts (Figure 3Bb). Immunoprecipitation of plasma-membrane and cytosolic fractions from human osteoclasts revealed a membrane location for the FSHR (Figure 3Bc).

FACS analysis of freshly isolated, uncultured bone-marrow precursors showed that the FSHR was expressed mainly in CD11b $^{+}$ osteoclast precursors (Figures 3Ca and 3Cb and Figure S1A) and persisted even after 2 days of culture with RANK-L (Figure 3Cc). Figure 3D shows that mature human osteoclasts after 8 days of culture with RANK-L labeled for FSHR, but Caco-2 cells did not (Figure 3D). Confocal microscopy showed strong membrane labeling of mature osteoclasts compared with the nonimmune control (Figures 3Ea and 3Eb, respectively). Thus, FSHRs are localized to the membrane surfaces of freshly isolated osteoclast precursors and mature osteoclasts.

Real-time PCR of primary murine osteoclasts showed that *FSHR* mRNA expression increased progressively up to 8-fold at 5 days post-RANK-L (Figure 3F). To study the regulation of FSHR expression by RANK-L, RAW-C3 cells were used in promoter-reporter assays. RANK-L increased the transcription of pBL(-1548) and pBL(-867) but not minimal length pBL(-99) (Figure 3G), suggesting that RANK-L directly regulates *FSHR* transcription.

FSH Enhances Osteoclast Differentiation and Bone Resorption

Because the absence of FSH action diminished bone resorption in vivo, we examined whether FSH directly

enhanced osteoclast differentiation and function. Osteoclastogenesis from human mononuclear cell precursors was stimulated in a concentration-dependent manner with significant effects at 3 ng/ml-FSH (Figures 4A and 4B). FSH similarly stimulated osteoclastogenesis in bone-marrow cultures from C57BL/6J and 129 mice and in RAW cell cultures (Figures 4C and 4D). LH (10 or 100 ng/ml) did not stimulate osteoclast differentiation in human or mouse cultures (Figure 4). Overall, the in vitro results are in keeping with the increased ex vivo TRAP labeling induced by FSH in calvarial bones (Figure 1J).

Figure 4E shows toluidine-blue-positive resorption pits formed by osteoclasts derived from human mononuclear cells. There was a concentration-dependent increase in the area degraded/total area (Figure 4Fa), paralleled by an increase in nuclear number in cells on plastic (Figure 4Fb), except at 30 ng/ml. This implied that, while in large part an increased multinucleated osteoclast number contributed to the stimulated resorption, a dissociation between genesis and function was observed at the highest concentration. To determine whether FSH enhanced the resorptive activity of individual osteoclasts, we measured the size of individual resorption pits, a parameter that is independent of the number of osteoclasts. FSH enhanced pit size significantly at all FSH concentrations (Figure 4G). LH or the LH/FSH secretagogue, GnRH, failed to affect either parameter (Figures 4E-4G).

We attempted to distinguish effects of FSH on the proliferation versus differentiation of osteoclast precursors. FSH did not affect precursor proliferation (Figure 4H) but stimulated expression of the differentiation marker TRAP (Figure 4I). We next sought to eliminate any interaction between FSH and the TSHR (Abe et al., 2003). FSH stimulated osteoclastogenesis in TSHR $^{-/-}$ but not in FSHR $^{-/-}$ cultures (Figure 4J), ruling out a role for the TSHR. As a further control, we overexpressed the FSHR in RAW-C3 cells and found evidence of augmented osteoclastogenesis and TRAP mRNA expression compared with vector-only controls (Figures 4Ka and 4Kb). Together, these data indicate that the FSH effects are mediated solely through the FSHR.

We next studied the effects of FSH on bone formation in calvarial cultures using ex vivo calcein labeling (modified

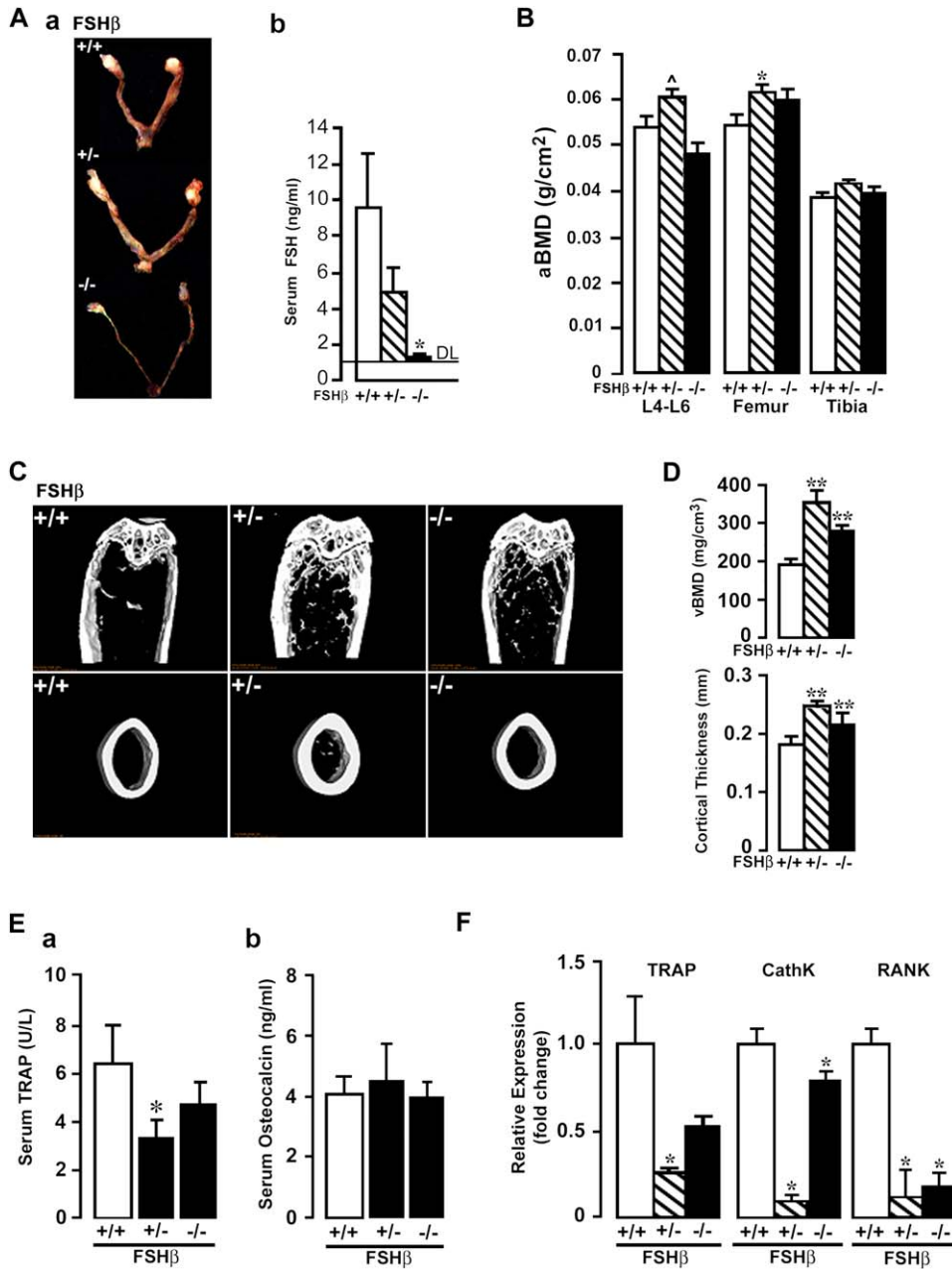


Figure 2. Increased Bone Mass in FSH β ^{+/-} and FSH β ^{-/-} Mice

(Aa) Hypogonadal FSH β ^{-/-} mice have hypoplastic thread-like uteri and atrophic ovaries, which are normal in eugonadal FSH β ^{+/-} mice.

(Ab) Serum FSH levels (n = 5 mice/group). Serum calcium, phosphate, and alkaline phosphatase are normal (not shown).

(B) Areal bone mineral density (aBMD) in 6-month-old mice. Mean \pm SEM, n = 4–5/group.

(C) Frontal (upper) and transverse (lower) μ CT sections of distal and midfemoral diaphyses.

(D) Volumetric BMD (vBMD) and cortical thickness at the distal and mid-diaphyses. Mean \pm SEM, n = 3 mice/group.

(Ea and Eb) Serum TRAP (U/L, [Ea]) and osteocalcin (ng/ml, [Eb]) levels. Mean \pm SEM, 9–16 mice/group.

(F) Real-time PCR for *TRAP*, *cathepsin K* (*CathK*), and *RANK* in bone marrow cells. Mean fold change from wt mice (\pm SEM, triplicate, pooled samples, normalized to *GAPDH*). $\Delta p = 0.07$, * $p < 0.05$, ** $p < 0.01$.

from Mundy et al., 1999). FSH did not increase calcein-labeled surfaces, whereas BMP-2 showed a dramatic 6-fold increase (Figure 5A). Consistent with this, we found

that FSH did not alter the formation of CFU-F or CFU-ob colonies (Figures 5B–5D). This result is not unexpected since mature osteoblasts do not express FSHRs

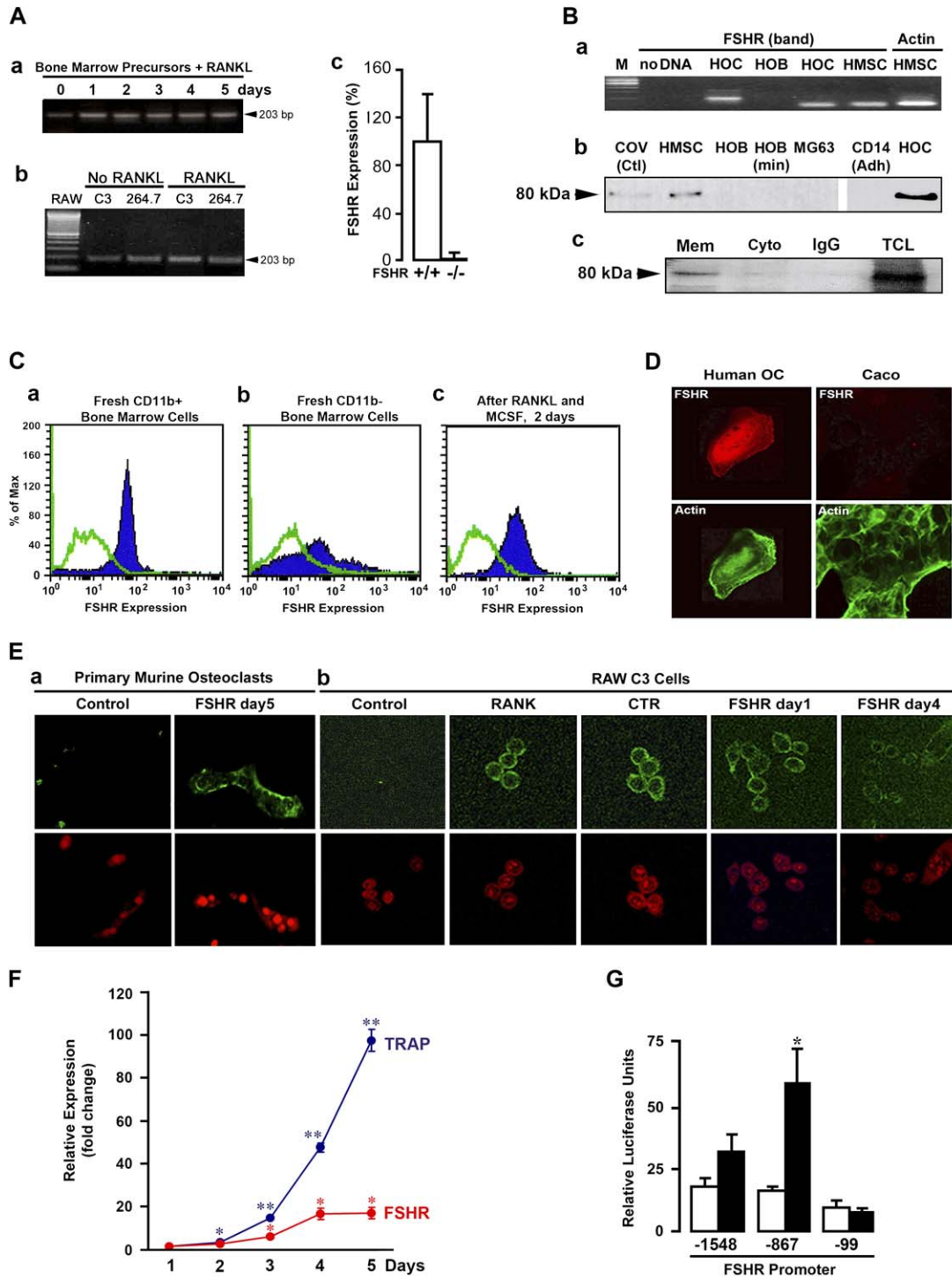


Figure 3. FSH Receptors on Osteoclasts and Osteoclast Precursors

(Aa and Ab) PCR bands for murine *FSHR* from cells undergoing osteoclastogenesis (days post-RANK-L, 60 ng/ml) or RAW264.7 and RAW-C3 cells at 2 days \pm RANK-L (60 ng/ml).

(Ac) Real-time PCR for *FSHR* mRNA in Ficoll-purified bone-marrow cells. % of wt \pm SD, normalized to mouse β_2 -microglobulin.

(Ba) RT-PCR bands using two primer sets for human *FSHR* mRNA noted in osteoclasts (HOC) and mesenchymal stem cells (HMSC) but not in osteoblasts (HOB).

(Bb) Western blot showing a human *FSHR* band in whole-cell lysates of COV34 ovarian granulosa cells (COV Ctl), HMSC, and HOC but not in quiescent or mineralizing (min) HOBs, MG63 cells, or adherent (Adh) CD14⁺ cells.

(Figures 3Ba and 3Bb) and is congruous with the lack of a bone formation defect and normal osteocalcin levels in FSH β and FSHR knockout mice (Figure 1Fb, Figure 2Eb, and Table 1).

However, as mesenchymal stem cells possess the FSHR (Figures 3Ba and 3Bb), the possibility remained that FSH could use osteoblast precursors/stromal cells to stimulate osteoclastogenesis. Figure 5E shows that cultures containing only CD11b⁺ cells, without stromal cells, mount a full osteoclastogenic response to FSH. We next examined directly whether wild-type stromal cells could rescue the expected loss of osteoclastogenesis in cocultures containing FSHR^{-/-} osteoclasts. Figure 5F shows that FSH did not stimulate osteoclastogenesis when wild-type stromal cells were cocultured with FSHR^{-/-} osteoclasts. This confirmed that pro-osteoclastogenic actions of FSH are mediated solely by the osteoclastic FSHR, with minimal, if any, contribution from stromal cells. In keeping with these findings, FSH did not stimulate RANK-L production in stromal cell cultures, while 1,25-D₃ did (Figure 5G). Together, the results suggest that FSH-induced osteoclastogenesis is exerted solely via CD11b⁺ cells.

FSH Signals via G_{i2 α} to Activate the MEK/Erk, NF- κ B, and Akt Pathways

Published data on ovarian cells demonstrate that the FSHR couples with a G_{s α} and elevates cAMP (Conti, 2002). However, similar to studies with luteal granulosa and Sertoli cells (e.g., Saltarelli, 1999; Sairam et al., 1996), we found that the osteoclastic FSHR couples to G_{i α} . CD11b⁺ osteoclast precursors expressed G_{i2 α} , with minimal, if any, expression of the other isoforms, G_{i1 α} and G_{i3 α} (Figure 6A). Consistent with the activation of an inhibitory G protein, FSH triggered a concentration-dependent reduction in cAMP levels (Figure 6B).

G_i activation is linked to the stimulation of the MEK/Erk pathway (Pace et al., 1995). G_{i2 α} activation in Sertoli cells by FSH enhances Erk1/2 phosphorylation (Crepieux et al., 2001). We therefore first examined whether FSH stimulated MAP kinase (MEK/Erk, JNK, and p38), Akt, and NF- κ B pathways. FSH stimulated Erk1/2, Akt, and I κ B α phosphorylation within 10 min with minimal to no effect on JNK or p38 (Figure 6C). Likewise, in human osteoclasts, Erk1/2 and Akt phosphorylation were enhanced by

2 and 20 min, respectively, (Figure 6D). FSH-induced Erk1/2 phosphorylation was associated with the nuclear localization of c-Fos (Figures 6D and 6E).

We next studied the role of G_{i2 α} by utilizing G_{i2 α} ^{-/-} cells. The nuclear localization of c-Fos in response to FSH was attenuated in G_{i2 α} ^{-/-} cells (Figure 6E). Additionally, the enhanced Erk1/2 and I κ B α phosphorylation seen with FSH in wild-type cells was absent in G_{i2 α} ^{-/-} cells (Figure 6F); this was in contrast to RANK-L, which activated both molecules (Figure 6F). Finally, while basal osteoclast formation in G_{i2 α} ^{-/-} cells was higher than in wild-type cells, the stimulatory effect of FSH on osteoclast formation was lost (Figure 6G). Together, the results established that G_{i2 α} was essential for the effects of FSH on Erk/c-Fos and NF- κ B signaling and osteoclast formation.

We next examined the importance of each downstream signaling pathway in mediating the FSH effect. A small molecule inhibitor of MEK1/2, U0126, abrogated the FSH-induced expression of *TRAP* at day 2 without affecting the RANK-L-induced *TRAP* elevation (Figure 6H). In contrast, in the presence of the JNK inhibitor SB600125, FSH still significantly increased *TRAP* expression, although the response magnitude was attenuated (Figure 6H). This response attenuation is in concordance with the minimal induction of JNK phosphorylation by FSH (Figure 6C). In contrast, the MEK inhibitors PD98059 and U0126 abrogated the effect of FSH to levels obtained in the presence of RANK-L alone (Figure 6I). Neither inhibitor impaired the osteoclastogenesis induced by RANK-L (Figure 6I and Figure S1B). We also quantitated the binding of p65 to a NF- κ B consensus sequence and found it to be enhanced significantly in response to FSH (Figure 6J). Together, the results established that the MEK/Erk and NF- κ B pathways contribute to the effect of FSH on osteoclast differentiation.

Finally, to examine whether the PI3-kinase/Akt pathway was involved, we (1) infected primary murine cells with an adenovirus expressing dominant-negative Akt (Akt^{dn}) and (2) treated the cells with LY294002, a PI3-kinase inhibitor. The stimulatory effect of FSH was lost with 5 moi Akt^{dn} and attenuated significantly with 2 moi Akt^{dn} (Figure 6K). Furthermore, LY294002 abolished FSH-induced increases in osteoclastogenesis (Figure 6I) and *TRAP* mRNA expression (Figure 6L). Together, the evidence establishes Akt as a mediator of FSH action.

(Bc) Whole-cell lysates (TCL) and plasma-membrane (Mem) and cytoplasmic (Cyto) fractions immunoprecipitated and then probed with anti-FSHR antibody.

(Ca–Cc) FACS showing FSHR expression (blue) in uncultured CD11b⁺ (Ca) and CD11b⁻ bone-marrow cells (Cb) and in cells 2 days post-RANK-L (100 ng/ml) (Cc). Green, isotype control.

(D) Immunolabeling of human osteoclasts or Caco-2 cells (Caco) with anti-FSHR antibody (60 ng/ml, upper panels). Bottom panels show phalloidin labeling.

(Ea and Eb) Immunolabeling of mature osteoclasts derived from bone-marrow (Ea) or RAW-C3 cells (Eb) using antibodies to RANK, calcitonin receptor (CTR), or FSHR (upper panels, green). Red, nuclear labeling of the same cells with propidium iodide.

(F) Real-time PCR for *FSHR* and *TRAP* mRNA in primary murine osteoclast precursors (RANK-L, 50 ng/ml). Mean fold change from day 1 normalized to *GAPDH* (\pm SEM). * p < 0.05, ** p < 0.01.

(G) Mean relative luciferase units (\pm SEM) in RAW-C3 cells transfected with full-length and deletion fragments of the *FSHR* promoter treated with RANK-L (filled bars) or vehicle (open bars) for 2 days. * p < 0.05; six separate experiments pooled.

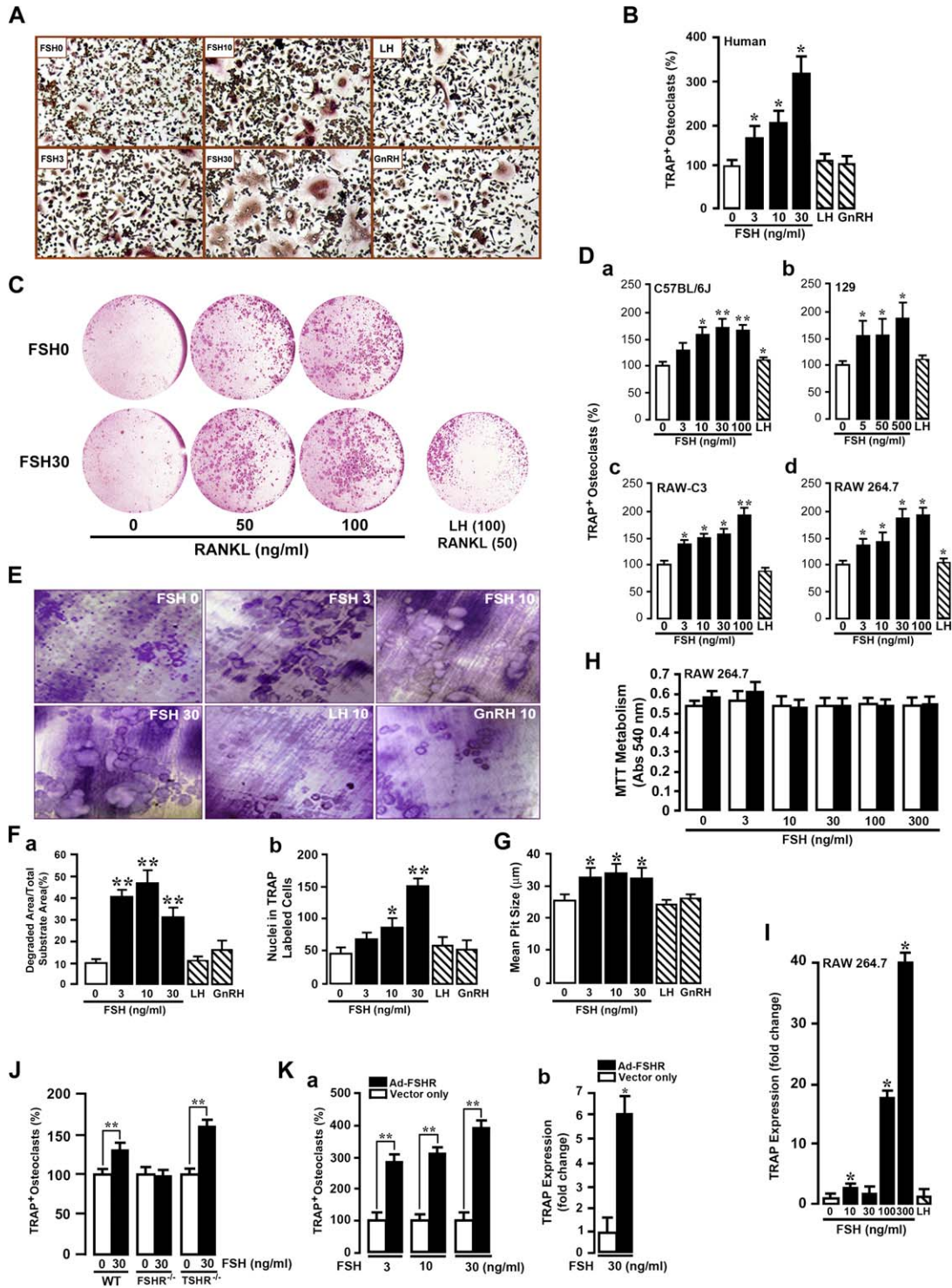


Figure 4. FSH Stimulates Osteoclastogenesis and Resorption

(A and B) Effect of FSH, LH (30 ng/ml), and GnRH (30 ng/ml) on TRAP-positive human osteoclast numbers (RANK-L, 60 ng/ml, 8 days). Results in (B) are expressed as % of 0 dose (\pm SEM, n = 4 wells/dose).

(C) Effect of FSH or LH on TRAP-positive osteoclast numbers.

(Da–Dd) Effect of FSH or LH (100 ng/ml) on TRAP-positive osteoclast numbers (\pm SEM) in 5-day cultures from C57/BL6J (Da) or 129 (Db) mouse strains or RAW-C3 (Dc) or RAW264.7 (Dd) cells (2–3 experiments/set; 3–5 wells/concentration).

(E) Light micrographs of toluidine-blue-stained resorption pits showing the effect of FSH, LH (10 ng/ml), and GnRH (10 ng/ml).

(F) Light micrographs of toluidine-blue-stained resorption pits showing the effect of FSH, LH (10 ng/ml), and GnRH (10 ng/ml).

DISCUSSION

This study determined whether FSH directly affects skeletal remodeling. We show that FSH stimulates the formation and function of osteoclasts *in vitro* and *in vivo*. These actions are exerted via a $G_{i2\alpha}$ -coupled FSHR that triggers the MEK/Erk, NF- κ B, and Akt pathways. A complete loss of FSH signaling in FSHR^{-/-} and FSH β ^{-/-} mice protects from bone loss despite severe hypogonadism. Haploinsufficiency of circulating FSH increases bone mass by reducing osteoclastic bone resorption in the presence of normal estrogen levels. This indicates a direct estrogen-independent action of FSH on the osteoclast.

FSH Is Necessary for Hypogonadal Bone Loss

The elevated bone resorption in hypogonadism arises mainly from increased osteoclast formation, a phenomenon that has been attributed to estrogen deficiency (Riggs *et al.*, 2002). However, it is unclear why hypogonadal mice deficient in α , β , or both estrogen receptors are not severely osteoporotic, while ovariectomized or aromatase null mice, which are similarly hypogonadal, experience profound bone loss (McCauley *et al.*, 2002; Windahl *et al.*, 2002; Lindberg *et al.*, 2001; Oz *et al.*, 2000, 2001). It also remains uncertain why ovariectomy plus hypophysectomy in rats causes less bone loss than ovariectomy alone (Yeh *et al.*, 1996, 1997). We find that both of these quandaries can be explained by differences in FSH levels. Ovariectomized or aromatase-deficient mice have high FSH levels (Britt *et al.*, 2001), while estrogen-receptor null mice have near normal levels of FSH (Couse *et al.*, 2003). Similarly, ovariectomy with hypophysectomy is associated with FSH deficiency, while ovariectomy alone causes FSH levels to increase (Clayton, 1993). Thus, irrespective of the nature or severity of estrogen deficiency, an intact pituitary and, more specifically from our results, high FSH levels are prerequisites for hypogonadal bone loss.

Because hypogonadal bone loss has been attributed solely to low estrogen in the past, a direct action of FSH on the skeleton has never been explored. We thus examined the *in vivo* effects of deleting FSH or its receptor on bone remodeling. As FSH promotes the differentiation of ovarian follicles and modulates estrogen secretion, both FSH β and FSHR null mice have atrophic ovaries and thread-like uteri, constituting evidence for profound estrogen deficiency (Dierich *et al.*, 1998; Danilovich *et al.*, 2000; Kumar *et al.*, 1997). We show that the absence of FSH ac-

tion protects both trabecular and cortical bone from the effects of hypogonadism, while ovariectomized controls expectedly lose bone. More importantly, haploinsufficient FSH β ^{+/-} mice that are eugonadal have an increased bone mass, suggesting a direct, estrogen-independent action of FSH on bone.

While hypogonadism from ovariectomy increases osteoclastic bone resorption *in vivo*, severely hypogonadal FSHR or FSH β null mice show decreased bone resorption. Although *in vivo* resorptive surfaces do not differ between FSHR^{-/-} and wild-type littermates, FSHR^{-/-} bone-marrow cell cultures show decreases in osteoclast formation and marker expression in response to RANK-L. This compensated defect in osteoclastogenesis unravels *in vivo* when FSHR^{-/-} calvaria are exposed to RANK-L.

In ligand-deficient FSH β ^{-/-} mice, *in vivo* resorption surfaces are reduced in contrast to FSHR^{-/-} mice. This attenuation is greater in eugonadal heterozygotic mice that have significantly lower serum TRAP levels and osteoclast marker expression. Reduced osteoclastic resorption in FSH β ^{+/-} eugonadal mice establishes that FSH modulates osteoclastogenesis independently of estrogen. That the FSH β or FSHR genotypes show no differences in serum osteocalcin levels or mean bone apposition rates excludes the possibility that increased bone formation contributes to the conserved bone mass.

FSH Directly Increases Osteoclastogenesis and Resorption

FSH stimulates osteoclastogenesis and bone resorption by acting on a $G_{i2\alpha}$ -coupled FSHR. We localized FSHRs to the surface of murine and human osteoclasts and their precursors. FSHRs were also present on mesenchymal stem cells but not on mature osteoblasts, raising the possibility that the enhanced osteoclastogenesis could be mediated via FSHRs on stromal cells. We find, however, that this is not the case. First, FSHR^{+/-} osteoblast precursors failed to rescue the abrogated osteoclastogenesis seen in cocultures with FSHR^{-/-} osteoclast precursors. In keeping with this, FSH induced a full osteoclastogenic response in purified CD11b⁺ cells, without the requirement of the CD11b⁻ fraction that contains stromal cells and lymphocytes. Finally, FSH did not enhance the secretion of RANK-L from stromal cell cultures. Taken together, these observations suggest that stromal cells and lymphocytes do not mediate FSH-induced osteoclastogenesis.

FSHRs are members of the TSHR/LHR/FSHR superfamily. We therefore sought to examine whether FSH

(F and G) Quantitation of degraded area/total substrate area (Fa), estimates of nuclear number in TRAP-labeled cells on plastic (Fb), and mean pit size (G) in response to FSH, LH (10 ng/ml), and GnRH (10 ng/ml) (\pm SEM; 4 slices/treatment, three experiments). * $p < 0.05$, ** $p < 0.01$.

(H) Lack of an effect of FSH on the proliferation of RAW264.7 cells with (closed bars) or without (open bars) RANK-L (60 ng/ml). Mean absorbance (Abs, \pm SEM) at 540 nm; two experiments pooled.

(I) Effect of FSH or LH (100 ng/ml) on *TRAP* mRNA expression in RAW264.7 cells by real-time PCR. Mean fold change (\pm SEM), triplicate measurements, normalized to *GAPDH*.

(J) Effect of FSH on TRAP-positive osteoclast numbers in wild-type (WT), FSHR^{-/-}, and TSHR^{-/-} cells. % of 0 dose (\pm SEM); $n = 5$ wells/treatment. (Ka and Kb) Effects of FSH on TRAP-positive osteoclast number (Ka) and *TRAP* mRNA by real-time PCR (Kb) in RAW-C3 cells infected with adenovirus containing the murine *FSHR* gene (closed bars) or empty vector (open bars). Mean \pm SEM, $n = 5$ wells/treatment; * $p < 0.05$, ** $p < 0.01$.

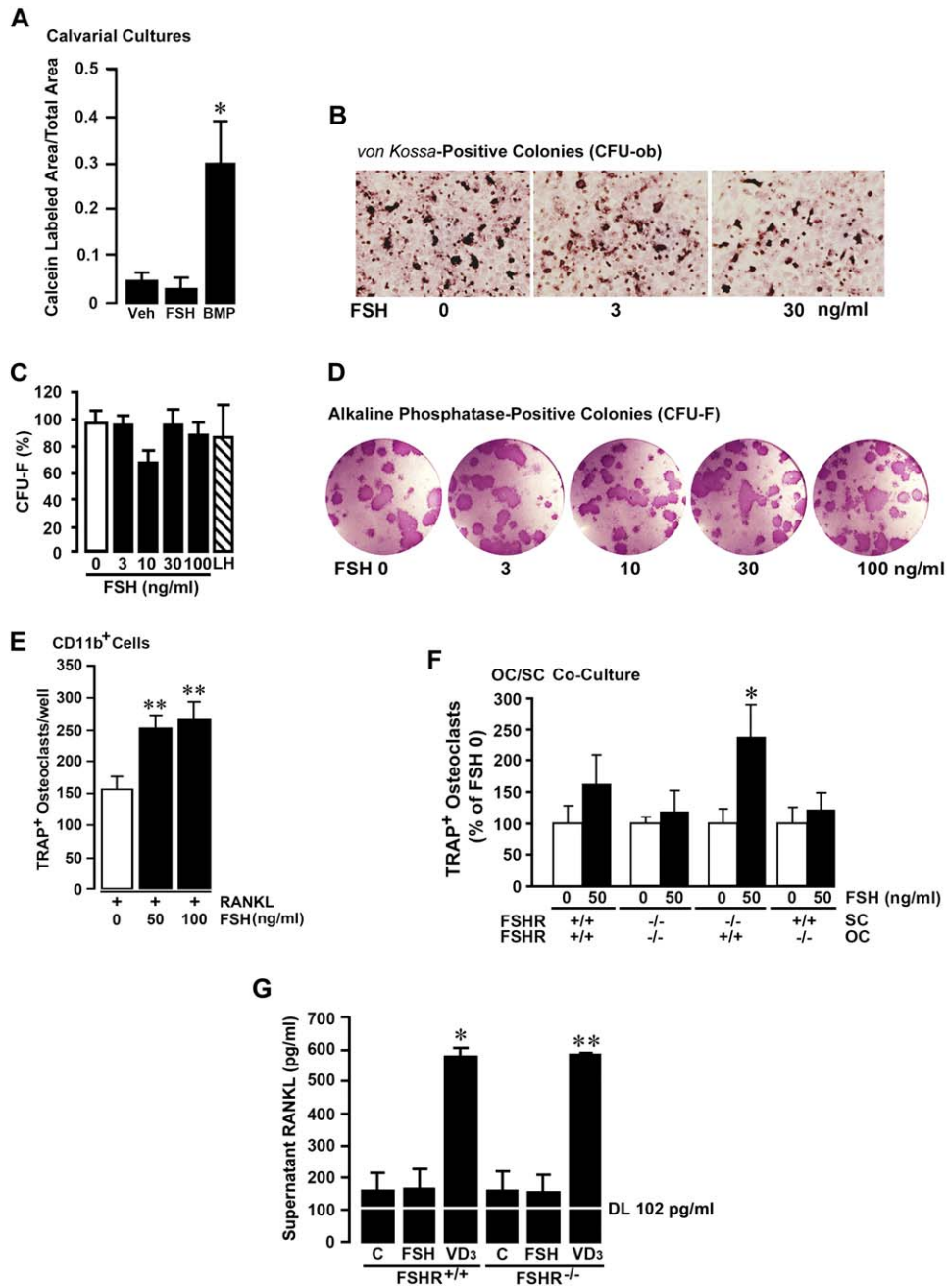


Figure 5. FSH Does Not Affect Osteoblasts

(A) Effect of FSH (100 ng/ml) and BMP-2 (200 ng/ml) on calcein-labeled area/total area in newborn mouse calvaria (modified from Mundy et al., 1999). Five fields measured from three or more sections; n = 5 mice/group.

(B–D) Lack of effect of FSH and/or LH (100 ng/ml) on von Kossa-positive CFU-ob (B) or alkaline-phosphatase-positive CFU-F (C and D) colonies. Results in (C) expressed as % of 0 dose (\pm SEM, 2 wells/concentration).

(E) Effect of FSH on TRAP-positive osteoclast numbers from CD11b-purified precursors (n = 6 wells/group). **p < 0.01.

(F) TRAP-positive osteoclast numbers in 10-day cocultures of FSHR^{-/-} and FSHR^{+/+} osteoclast precursors with stromal cells and 1,25-D₃ (10⁻⁸ M). % of 0 FSH \pm SEM. *p < 0.05.

(G) Effect of FSH (50 ng/ml) or 1,25-D₃ (VD₃, 10⁻⁸ M) on RANK-L (pg/ml) production (DL, detection limit). *p < 0.05, **p < 0.01; comparisons with 0 dose = "C."

displayed a weak antagonism to the TSHR, the stimulation of which inhibits osteoclastogenesis (Abe et al., 2003). We find that FSH elicits a full osteoclastogenic response in TSHR^{-/-} cultures, ruling out a role for TSHRs. We further established specificity by showing enhanced osteoclastogenesis in FSHR-overexpressing cultures.

While FSH stimulates osteoclastic bone resorption, it does not stimulate osteoblastic bone formation. CFU-F and CFU-ob formation were unaffected by FSH. Likewise, consistent with absent FSHRs on mature osteoblasts, calvarial bone formation remained unaltered with FSH, while it was enhanced with BMP-2. Moreover, serum osteocalcin levels remained unchanged when either FSH β or the FSHR was deleted, even in FSH β ^{+/-} mice with high bone mass. Finally, the mean bone apposition rate remains unchanged across the FSH β and FSHR genotypes. Overall, therefore, FSH does not appear to stimulate osteoblastic bone formation.

We find that osteoclastic FSHRs are coupled to G_{i2 α} , the major G_i isoform in CD11b⁺ osteoclast precursors. FSH-induced decreases in cAMP levels attest to this coupling. Whereas similar coupling of the FSHR to G_i has been noted in luteal granulosa and Sertoli cells (Saltarelli, 1999; Sairam et al., 1996), FSH actions in ovarian cells are mediated via G_{s α} (Conti, 2002).

FSH activates three known osteoclastogenic pathways by rapidly enhancing the phosphorylation of Erk1/2, I κ B α , and Akt (Teitelbaum, 2000). The effects of FSH on osteoclastogenesis, Erk1/2, and I κ B α activation and c-Fos nuclear localization were all abrogated in G_{i2 α} ^{-/-} cells. This suggests that Erk1/2, c-Fos, and I κ B α are downstream of G_{i2 α} . Consistent with this, FSH-induced increases in osteoclastogenesis were abrogated in G_{i2 α} ^{-/-} cells, although an elevation of osteoclast formation was noted in these cultures. It is, however, unlikely that this elevation arises from alterations in RANK-L-induced signaling pathways, as Erk and I κ B α phosphorylation in response to RANK-L remain unaffected in G_{i2 α} ^{-/-} cells. It would be interesting to examine whether G_{i2 α} regulates the generation of hematopoietic precursors to account for the in vitro phenotype.

We also find that FSH-induced osteoclast differentiation is attenuated by MEK inhibitors but not by a JNK inhibitor, indicating that the MEK/Erk pathway is essential. This is in contrast to TSH and estrogen, which both reduce JNK activation to inhibit osteoclastogenesis (Shevde et al., 2000; Abe et al., 2003). The osteoclastogenic action of FSH was also abrogated with dominant-negative Akt or a PI3-kinase inhibitor. While we have not similarly used an NF- κ B inhibitor, we find that FSH increases p65 transactivation. Overall, therefore, FSH activates Erk1/2, Akt, and NF- κ B but not p38 and JNK to stimulate the osteoclast formation.

FSH Regulates Bone Remodeling in Health and Disease

That FSH stimulates bone resorption may have physiological and pathophysiological implications. Onset of the fol-

licular phase in the menstrual cycle marks a sharp rise in FSH levels. At this time, markers of bone resorption are high, despite modest elevations in estrogen levels that would be expected to lower bone resorption (Gorai et al., 1995; Chiu et al., 1999; Zittermann et al., 2000). As estrogen levels peak in the late follicular stage, bone formation markers such as osteocalcin begin to rise, likely due to the anabolic actions of estrogen (Gorai et al., 1995). We speculate therefore that the respective remodeling processes, resorption and formation, are stimulated in sequence by FSH followed by estrogen during the estrous cycle.

Pathophysiologically, the results suggest that the bone loss during early menopause and in hypogonadism, which has been attributed solely to declining sex hormone levels, may result at least in significant part from elevated circulating FSH. There is no correlation between the serum levels of estrogen and markers of bone resorption (Riggs et al., 2002; Khosla et al., 1998). Instead, there is a strong correlation between rising serum FSH levels and elevated bone resorption markers in early menopause (Sowers et al., 2003). Furthermore, BMD is lower in hypergonadotrophic amenorrheic women with high circulating FSH compared with amenorrheic females with normal or low FSH levels (Devleta et al., 2004). Postmenopausal serum FSH levels (Padmanabhan et al., 1989) correspond to concentrations that stimulate human osteoclasts in vitro. Finally, reduced FSH levels and increased BMD correlate well following estrogen replacement therapy (Kawai et al., 2004). Thus, we speculate that a high circulating FSH causes postmenopausal and hypogonadal osteoporosis.

EXPERIMENTAL PROCEDURES

FSHR, FSH β , and G_{i2 α} null mice were 129T2svEmsJ, C57BL/6Jx129, and C57BL/6Jx129Sv backgrounds, respectively. Areal BMD was measured using PIXImus (Lunar-GE). Volumetric BMD was measured using eXplore SP μ CT (GE). A 1 mm volume of interest (voi) was selected to enclose the endocortical surface, and parameters were quantified using Advanced Bone Analysis software (GE). A voi of 2 \times 2 \times 0.5 mm was selected at the center of the middiaphysis to measure cortical thickness by MatLab v.6.5 (MathWorks). Histomorphometry was performed on frozen sections following calcein labeling per Abe et al. (2003). Serum FSH was measured using an RIA (detection limit [DL] = 1.17 ng/ml). Serum TRAP and osteocalcin were measured by ELISAs (SBA Sciences, TR103, DL = 0.1 IU/l for TRAP; BTI Biomedical Technologies, BT470, DL = 1.0 ng/ml for osteocalcin).

Murine bone-marrow and RAW cell cultures were performed as described by Wu et al. (2003). For osteoblast/osteoclast cocultures, stromal cells were first exposed to an anti-c-Fms antibody (2 μ g/ml) for 2 weeks to eliminate osteoclast precursors and then cocultured with Ficoll-purified cells and 1,25-D₃ (10⁻⁸ M) for 10 days. The MTT metabolism assay on RAW264.7 cells was carried out per manufacturer (ATCC). For adenoviral infections, RAW-C3 or bone-marrow cells were incubated with Ad5-FSHR or Ad-Akt^{dn} for 24 hr followed by RANK-L and FSH for 5 days. Resorptive activity of osteoclasts was examined using the standard pit assay (Sun et al., 2003). To assess bone resorption ex vivo, we modified an in vivo method by Novack et al. (2003). Calvaria from FSHR^{-/-} and wild-type mice were incubated in α -MEM for 48 hr with RANK-L, FSH, or BMP. Medullary bone surface was labeled for TRAP using α -naphthyl phosphate substrate before morphometric quantitation as a proportion of total surface. CFU-F

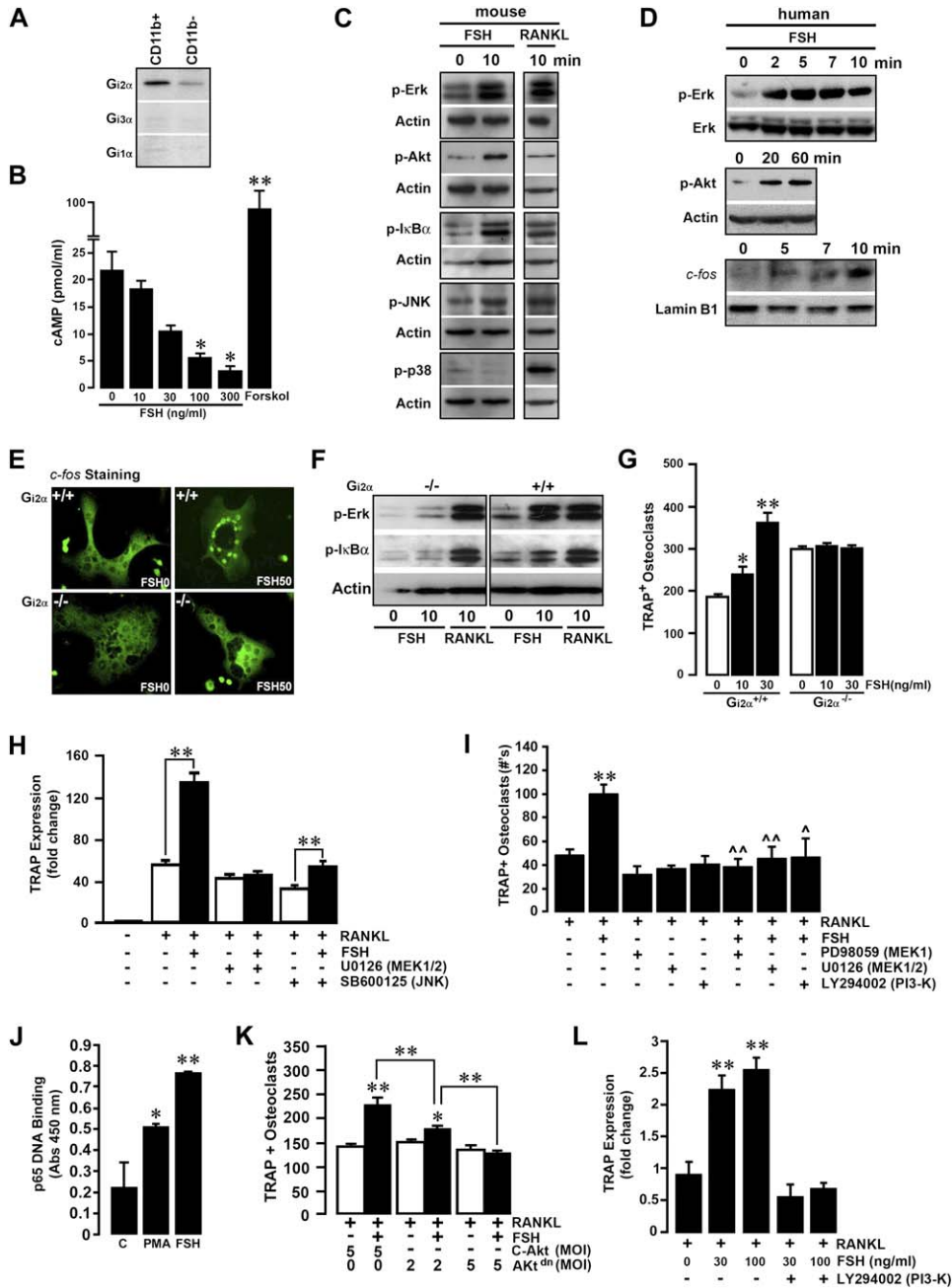


Figure 6. FSH Activates Erk, Akt, and IκBα via Gi_{2α}

(A) Western blots of CD11b⁺ and CD11b⁻ cells probed with antibodies to the G_{i2α} isoforms 1, 2, and 3.
 (B) Effect of FSH and forskolin (Forskol, 10 μM) on cAMP levels in osteoclast cultures. Mean ± SEM (repeated twice). **p < 0.01, *p < 0.05.
 (C and D) Western blots of phosphorylated (p-) Erk1/2, Akt, IκBα, JNK, or p38 levels or nuclear c-Fos levels in murine (C) or human (D) osteoclast precursors in response to FSH or RANK-L (50 ng/ml each).
 (E) Epifluorescence microscopy showing c-Fos localization to nuclei in mouse osteoclasts in response to FSH (50 ng/ml).
 (F) Western blots showing p-Erk1/2 and p-IκBα at 10 min in response to FSH or RANK-L (50 ng/ml each).
 (G) Effect of FSH on TRAP-positive osteoclast formation (RANK-L, 30 ng/ml). Mean ± SEM; n = 6 wells/treatment. *p < 0.05, **p < 0.01.
 (H) Real-time PCR showing the effect of the MEK1/2 or JNK inhibitors U0126 or SB600125 (0.5 μM each) on TRAP mRNA in 2-day cultures (RANK-L ± FSH, 50 ng/ml each). Mean fold change ± SEM versus no RANK-L, triplicate, normalized with mouse β₂-microglobulin, **p < 0.01.
 (I) Effect of MEK inhibitors PD98059 (5 μM) and U0126 (0.5 μM) or the PI3-kinase inhibitor LY294002 (0.5 μM) on TRAP-positive osteoclast numbers in response to 30 ng/ml FSH (RANK-L, 100 ng/ml). Mean ± SEM; three experiments; n = 10 wells. Comparisons with RANK-L alone (**p < 0.01) or with RANK-L + FSH (Δp < 0.05, ΔΔp < 0.01).
 (J) p65 DNA Binding (Abs 450 nm) in response to PMA and FSH.
 (K) TRAP + Osteoclasts in response to FSH with Akt inhibitor (Akt^{dn} MOI).
 (L) TRAP Expression (fold change) in response to FSH with Akt inhibitor (Akt^{dn} MOI).

and CFU-ob formation was examined by a method described by Abe et al. (2000). For examining bone formation *ex vivo*, newborn calvaria were incubated with calcein for 5 days. Frozen sections were analyzed for calcein labels relative to total bone area (Fovea Pro, Reindeer Graphics, Asheville, NC, USA).

Human CD14 monocytes were cultured for 8 days and TRAP stained as previously described (Blair et al., 2004). Human osteoblasts (NHOST cells, Cambrex) were cultured with ascorbate-2-glycerol phosphate for 3 weeks. Plasma membranes were isolated by a sucrose gradient centrifugation method described by Sun et al. (1999). For resorption assays, CD14 monocytes were plated for 15 days with M-CSF and RANK-L on dentine slices that were subsequently toluidine blue stained. Total degraded area/total area (a combined measure of osteoclast differentiation and bone resorption) and the size of individual pits on 4–12 surfaces was estimated by morphometry. In parallel, the cells were plated on plastic and then TRAP labeled (above) for nuclear counts.

Flow cytometry was performed using FACSCalibur and CellQuest/FlowJo. Osteoclasts were immunostained for confocal microscopy using a protocol by Sun et al. (2002). Antibodies were human anti-FSHR (Zymed); CD11b, c-Fms, and c-Kit (BD Biosciences); c-Fos (Santa Cruz); and p-Erk1/2, Erk, p-JNK, p-p38, p-I κ B α , and p-Akt (Cell Signaling).

DNA binding of p65 was examined using whole-cell extracts from primary cells treated with vehicle, PMA (1 mM), or FSH (50 ng/ml) for 10 min without RANK-L. Extracts were assayed in NF- κ B consensus sequence (GGGGTATTCC) coated 96-well plates (Clonetech, 631930) per manufacturer. PCR and real-time PCR were carried out by a method in Zhu et al. (2005) utilizing ABI Prism 7000 or 7900HT. Each transcript was assayed 3 times, and cDNA loading was normalized to human or murine *GAPDH* or murine β_2 -microglobulin.

A pBL(-1548) plasmid with a 1.5 kb mouse FSHR promoter fused with luciferase (from Dr. Ilpo Huhtaniemi) was used to prepare deletion mutants that were transfected into RAW cells. Luciferase activity was measured using a TopCount NXT Microplate Luminescence Counter (Packard) and Stop/Glo-measured Renilla luciferase.

Statistics by Student's *t* test (Excel) compared groups for significant differences at $p < 0.05$.

Supplemental Data

Supplemental Data include one figure and one table and can be found with this article online at <http://www.cell.com/cgi/content/full/125/2/247/DC1/>.

ACKNOWLEDGMENTS

We gratefully acknowledge support from the NIH and VA: AG14907, DK70526, and AG23176 to M.Z.; AR41210 to M.B.S.; AG12951 and AR47700 to H.C.B.; and VA Merit Review to M.Z., B.S.M., and H.C.B. M.B.S. and M.R.S. acknowledge NASA and the Canadian Institutes of Health Research. We thank Professors Iain MacIntyre, Terry Davies, and Ravi Iyengar for discussion.

Received: March 9, 2005

Revised: September 2, 2005

Accepted: January 23, 2006

Published: April 20, 2006

REFERENCES

- Abe, E., Yamamoto, M., Taguchi, Y., Lecka-Czernik, B., O'Brien, C.A., Economides, A.N., Stahl, N., Jilka, R.L., and Manolagas, S.C. (2000). Essential requirement of BMPs-2/4 for both osteoblast and osteoclast formation in murine bone marrow cultures from adult mice: antagonism by noggin. *J. Bone Miner. Res.* *15*, 663–673.
- Abe, E., Marians, R.C., Yu, W., Wu, X.B., Ando, T., Li, Y., Iqbal, J., Eldeiry, L., Rajendren, G., Blair, H.C., et al. (2003). TSH is a negative regulator of skeletal remodeling. *Cell* *115*, 151–162.
- Blair, H.C., Borysenko, C.W., Villa, A., Schlesinger, P.H., Kalla, S.E., Yaroslavskiy, B.B., Garcia-Palacios, V., Oakley, J.I., and Orchard, P.J. (2004). In vitro differentiation of CD14 cells from osteopetrotic subjects: contrasting phenotypes with TCIRG1, CLCN7, and attachment defects. *J. Bone Miner. Res.* *19*, 1329–1338.
- Britt, K.L., Drummond, A.E., Dyson, M., Wreford, N.G., Jones, M.E., Simpson, E.R., and Findlay, J.K. (2001). The ovarian phenotype of the aromatase knockout (ArKO) mouse. *J. Steroid Biochem. Mol. Biol.* *79*, 181–185.
- Cenci, S., Toraldo, G., Weitzmann, M.N., Roggia, C., Gao, Y., Qian, W.P., Sierra, O., and Pacifici, R. (2003). Estrogen deficiency induces bone loss by increasing T cell proliferation and lifespan through IFN- γ -induced class II transactivator. *Proc. Natl. Acad. Sci. USA* *100*, 10405–10410.
- Chiu, K.M., Ju, J., Mayes, D., Bacchetti, P., Weitz, S., and Arnaud, C.D. (1999). Changes in bone resorption during the menstrual cycle. *J. Bone Miner. Res.* *14*, 609–615.
- Clayton, R.N. (1993). Regulation of gonadotrophin subunit gene expression. *Hum. Reprod.* *8*, 29–36.
- Conti, M. (2002). Specificity of the cyclic adenosine 3',5'-monophosphate signal in granulosa cell function. *Biol. Reprod.* *67*, 1653–1661.
- Couse, J.F., Yates, M.M., Walker, V.R., and Korach, K.S. (2003). Characterization of the hypothalamic-pituitary-gonadal axis in estrogen receptor (ER) null mice reveals hypergonadism and endocrine sex reversal in females lacking ER α but not ER β . *Mol. Endocrinol.* *17*, 1039–1053.
- Crepieux, P., Marion, S., Martinat, N., Fafeur, V., Vern, Y.L., Kerboeuf, D., Guillou, F., and Reiter, E. (2001). The ERK-dependent signalling is stage-specifically modulated by FSH, during primary Sertoli cell maturation. *Oncogene* *20*, 4696–4709.
- Danilovich, N., Babu, P.S., Xing, W., Gerdes, M., Krishnamurthy, H., and Sairam, M.R. (2000). Estrogen deficiency, obesity, and skeletal abnormalities in follicle-stimulating hormone receptor knockout (FORKO) female mice. *Endocrinology* *141*, 4295–4308.
- Devleta, B., Adem, B., and Senada, S. (2004). Hypergonadotropic amenorrhea and bone density: new approach to an old problem. *J. Bone Miner. Metab.* *22*, 360–364.
- Dierich, A., Sairam, M.R., Monaco, L., Fimia, G.M., Gansmuller, A., LeMeur, M., and Sassone-Corsi, P. (1998). Impairing follicle-stimulating hormone (FSH) signaling in vivo: targeted disruption of the FSH receptor leads to aberrant gametogenesis and hormonal imbalance. *Proc. Natl. Acad. Sci. USA* *95*, 13612–13617.
- Gorai, I., Chaki, O., Nakayama, M., and Minaguchi, H. (1995). Urinary biochemical markers for bone resorption during the menstrual cycle. *Calcif. Tissue Int.* *57*, 100–104.

(J) p65 binding to a consensus NF- κ B sequence 10 min following vehicle, PMA (1 mM), or FSH (50 ng/ml) (no RANK-L). Mean absorbance (Abs) at 450 nm \pm SD ($n = 4$ wells/treatment, repeated twice).

(K) Effect of FSH (30 ng/ml) on TRAP-positive osteoclast numbers in cultures infected with empty adenovirus vector (C-Akt) or dominant-negative Akt (Akt^{dn}) (RANK-L, 30 ng/ml). Mean \pm SEM; $n = 6$ wells/treatment; * $p < 0.05$, ** $p < 0.01$.

(L) Real-time PCR showing the effect of LY294002 on basal or stimulated TRAP mRNA in 2-day cultures. Mean fold change \pm SEM, triplicate measurements, normalized to *GAPDH*, ** $p < 0.01$.

- Kawai, H., Furuhashi, M., and Suganuma, N. (2004). Serum follicle-stimulating hormone level is a predictor of bone mineral density in patients with hormone replacement therapy. *Arch. Gynecol. Obstet.* 269, 192–195.
- Khosla, S., Melton, L.J., 3rd, Atkinson, E.J., O'Fallon, W.M., Klee, G.G., and Riggs, B.L. (1998). Relationship of serum sex steroid levels and bone turnover markers with bone mineral density in men and women: a key role for bioavailable estrogen. *J. Clin. Endocrinol. Metab.* 83, 2266–2274.
- Kumar, T.R., Wang, Y., Lu, N., and Matzuk, M.M. (1997). Follicle stimulating hormone is required for ovarian follicle maturation but not male fertility. *Nat. Genet.* 15, 201–204.
- Lindberg, M.K., Alatalo, S.L., Hallee, J.M., Mohan, S., Gustafsson, J.A., and Ohlsson, C. (2001). Estrogen receptor specificity in the regulation of the skeleton in female mice. *J. Endocrinol.* 171, 229–236.
- Lindsay, R. (2004). Hormones and bone health in postmenopausal women. *Endocrine* 24, 223–230.
- Manolagas, S.C., and Jilka, R.L. (1995). Bone marrow, cytokines, and bone remodeling. Emerging insights into the pathophysiology of osteoporosis. *N. Engl. J. Med.* 332, 305–311.
- McCauley, L.K., Tozum, T.F., and Rosol, T.J. (2002). Estrogen receptors in skeletal metabolism: lessons from genetically modified models of receptor function. *Crit. Rev. Eukaryot. Gene Expr.* 12, 89–100.
- Minegishi, T., Nakamura, K., Takakura, Y., Ibuki, Y., Igarashi, M., and Minegishi, T. (1991). Cloning and sequencing of human FSH receptor cDNA. *Biochem. Biophys. Res. Commun.* 175, 1125–1130.
- Mundy, G., Garrett, R., Harris, S., Chan, J., Chen, D., Rossini, G., Boyce, B., Zhao, M., and Gutierrez, G. (1999). Stimulation of bone formation in vitro and in rodents by statins. *Science* 286, 1946–1949.
- Novack, D.V., Yin, L., Hagen-Stapleton, A., Schreiber, R.D., Goeddel, D.V., Ross, F.P., and Teitelbaum, S.L. (2003). The I κ B function of NF- κ B2 p100 controls stimulated osteoclastogenesis. *J. Exp. Med.* 198, 771–781.
- Oz, O.K., Zerwekh, J.E., Fisher, C., Graves, K., Nanu, L., Millsaps, R., and Simpson, E.R. (2000). Bone has a sexually dimorphic response to aromatase deficiency. *J. Bone Miner. Res.* 15, 507–514.
- Oz, O.K., Hirasawa, G., Lawson, J., Nanu, L., Constantinescu, A., Antich, P.P., Mason, R.P., Tsyganov, E., Parkey, R.W., Zerwekh, J.E., and Simpson, E.R. (2001). Bone phenotype of the aromatase deficient mouse. *J. Steroid Biochem. Mol. Biol.* 79, 49–59.
- Pace, A.M., Faure, M., and Bourne, H.R. (1995). Gi2-mediated activation of the MAP kinase cascade. *Mol. Biol. Cell* 6, 1685–1695.
- Padmanabhan, V., Sonstein, J., Olton, P.L., Nippoldt, T., Menon, K.M., Marshall, J.C., Kelch, R.P., and Beitins, I.Z. (1989). Serum bioactive follicle-stimulating hormone-like activity increases during pregnancy. *J. Clin. Endocrinol. Metab.* 69, 968–977.
- Prior, J.C. (1998). Perimenopause: the complex endocrinology of the menopausal transition. *Endocr. Rev.* 19, 397–428.
- Riggs, B.L., Khosla, S., and Melton, L.J., 3rd. (2002). Sex steroids and the construction and conservation of the adult skeleton. *Endocr. Rev.* 23, 279–302.
- Robker, R.L., and Richards, J.S. (1998). Hormonal control of the cell cycle in ovarian cells: proliferation vs differentiation. *Biol. Reprod.* 59, 476–482.
- Roggia, C., Gao, Y., Cenci, S., Weitzmann, M.N., Toraldo, G., Isaia, G., and Pacifici, R. (2001). Up-regulation of TNF-producing T cells in the bone marrow: a key mechanism by which estrogen deficiency induces bone loss in vivo. *Proc. Natl. Acad. Sci. USA* 98, 13960–13965.
- Sairam, M.R. (1999). Gonadotropins: overview. In *Encyclopedia of Reproduction*, E. Knobil and J.D. Niell, eds. (New York: Academic Press, Inc.), pp. 552–565.
- Sairam, M.R., Jiang, L.G., Khan, H., and Yarney, T.A. (1996). Follitropin signal transduction: Alternative splicing of the FSH receptor gene produces a dominant negative form of receptor which inhibits hormone action. *Biochem. Biophys. Res. Commun.* 226, 717–722.
- Saltarelli, D. (1999). Heterotrimeric Gi/o proteins control cyclic AMP oscillations and cytoskeletal structure assembly in primary human granulosa-lutein cells. *Cell. Signal.* 11, 415–433.
- Shevde, N.K., Bendixen, A.C., Dienger, K.M., and Pike, J.W. (2000). Estrogens suppress RANK ligand-induced osteoclast differentiation via a stromal cell independent mechanism involving c-Jun repression. *Proc. Natl. Acad. Sci. USA* 9, 7829–7834.
- Sowers, M.R., Greendale, G.A., Bondarenko, I., Finkelstein, J.S., Cauley, J.A., Neer, R.M., and Ettinger, B. (2003). Endogenous hormones and bone turnover markers in pre- and perimenopausal women: SWAN. *Osteoporos. Int.* 14, 191–197.
- Srivastava, S., Toraldo, G., Weitzmann, M.N., Cenci, S., Ross, F.P., and Pacifici, R. (2001). Estrogen decreases osteoclast formation by down-regulating receptor activator of NF- κ B ligand (RANKL)-induced JNK activation. *J. Biol. Chem.* 276, 8836–8840.
- Stepnick, L.S. (2004). The frequency of bone disease. In *Bone Health and Osteoporosis: A Report of the Surgeon General*, J.A. McGowan, L.G. Raisz, A.S. Noonan, and A.L. Elderkin, eds. (Washington, DC: Office of the US Surgeon General), pp. 68–87.
- Sun, L., Adebajo, O.A., Moonga, B.S., Corisdeo, S., Anandatheerthavarada, H.K., Biswas, G., Arakawa, T., Hakeda, Y., Koval, A., Sodam, B., et al. (1999). CD38/ADP-ribosyl cyclase: a new role in the regulation of osteoclastic bone resorption. *J. Cell Biol.* 146, 1161–1172.
- Sun, L., Adebajo, O.A., Koval, A., Anandatheerthavarada, H.K., Iqbal, J., Wu, X.Y., Moonga, B.S., Wu, X.B., Biswas, G., Bevis, P.J., et al. (2002). A novel mechanism for coupling cellular intermediary metabolism to cytosolic Ca²⁺ signaling via CD38/ADP-ribosyl cyclase, a putative intracellular NAD⁺ sensor. *FASEB J.* 16, 302–314.
- Sun, L., Iqbal, J., Dolgilevich, S., Yuen, T., Wu, X.B., Moonga, B.S., Adebajo, O.A., Bevis, P.J., Lund, F., Huang, C.L., et al. (2003). Disordered osteoclast formation and function in a CD38 (ADP-ribosyl cyclase)-deficient mouse establishes an essential role for CD38 in bone resorption. *FASEB J.* 17, 369–375.
- Teitelbaum, S.L. (2000). Bone resorption by osteoclasts. *Science* 289, 1504–1508.
- Windahl, S.H., Andersson, G., and Gustafsson, J.A. (2002). Elucidation of estrogen receptor function in bone with the use of mouse models. *Trends Endocrinol. Metab.* 13, 195–200.
- Wu, X.B., Li, Y., Schneider, A., Yu, W., Rajendren, G., Iqbal, J., Yamamoto, M., Alam, M., Brunet, L.J., Blair, H.C., et al. (2003). Impaired osteoblastic differentiation, reduced bone formation, and severe osteoporosis in noggin-overexpressing mice. *J. Clin. Invest.* 112, 924–934.
- Yeh, J.K., Chen, M.M., and Aloia, J.F. (1996). Ovariectomy-induced high turnover in cortical bone is dependent on pituitary hormone in rats. *Bone* 18, 443–450.
- Yeh, J.K., Chen, M.M., and Aloia, J.F. (1997). Effects of 17 beta-estradiol administration on cortical and cancellous bone of ovariectomized rats with and without hypophysectomy. *Bone* 20, 413–420.
- Zaidi, M., Alam, A.S., Shankar, V.S., Bax, B.E., Bax, C.M.R., Moonga, B.S., Bevis, P.J.R., Stevens, C.R., Blake, D.R., Pazianas, M., and Huang, C.L.-H. (1993). Cellular biology of bone resorption. *Biol. Rev. Camb. Philos. Soc.* 68, 197–264.
- Zhu, L.L., Zaidi, S., Moonga, B.S., Troen, B.R., and Sun, L. (2005). RANK-L induces the expression of NFATc1, but not of NF κ B subunits during osteoclast formation. *Biochem. Biophys. Res. Commun.* 326, 131–135.
- Zittermann, A., Schwarz, I., Scheld, K., Sudhop, T., Berthold, H.K., von Bergmann, K., van der Ven, H., and Stehle, P. (2000). Physiologic fluctuations of serum estradiol levels influence biochemical markers of bone resorption in young women. *J. Clin. Endocrinol. Metab.* 85, 95–101.